THE JOURNAL OF PHYSICAL CHEMISTRY B

Article

pubs.acs.org/JPCB

Formation of Hybrid Hydrogels Consisting of Tripeptide and Different Silver Nanoparticle-Capped Ligands: Modulation of the Mechanical Strength of Gel Phase Materials

Jayanta Nanda, Bimalendu Adhikari, Shibaji Basak, and Arindam Banerjee*

Department of Biological Chemistry, Indian Association of Cultivation of Science, Jadavpur, Kolkata- 700032, India

Supporting Information

ABSTRACT: An N-terminally Boc (*tert*-butyloxycarbonyl) group-protected synthetic tripeptide (Boc-Phe-Phe-Ala−OH) has been found to form a translucent hydrogel in basic aqueous medium. This hydrogel material has been characterized using field emission scanning electron microscopy (FE-SEM), transmission electron microscopy (TEM), Fourier transformed infrared spectroscopy, differential scanning calorimetric, X-ray diffraction (XRD), and rheological studies. FE-SEM and TEM studies have revealed the formation of a nanofibrillar network structure upon gelation. Thiol (-SH) containing ligands (amino acid/peptide) have been used to stabilize small silver nanoparticles (AgNPs), and these thiol-capped silver nanoparticles have been incorporated into this hydrogel to prepare hybrid hydrogels. Morphological study of silver nanoparticles containing a hybrid hydrogel (using TEM experiments) has indicated the nice fabrication of AgNPs along the gel nanofibers. Fabrication of nanoparticles upon the gel nanofibers is due to noncovalent interactions between the capping ligands of the nanoparticles and the peptide-based hydrogel nanofibers. Rheological investigations of these hybrid hydrogels have shown the weakening of the mechanical strength of the hydrogel after incorporation of AgNPs within the native hydrogel system. Our studies have vividly shown the dependence of the elastic modulus (G') and yield stress (σ_y) on three factors: (a) the nature of the stabilizing ligands used for AgNPs, (b) the size of the AgNPs, and (c) the amount of AgNPs used for the preparation of hybrid hydrogel systems. Modulation of the mechanical strength of the hybrid hydrogel can be successfully achieved by varying these above-mentioned factors. This modulation of the mechanical properties keeps a future promise to make tunable soft materials with interesting properties.

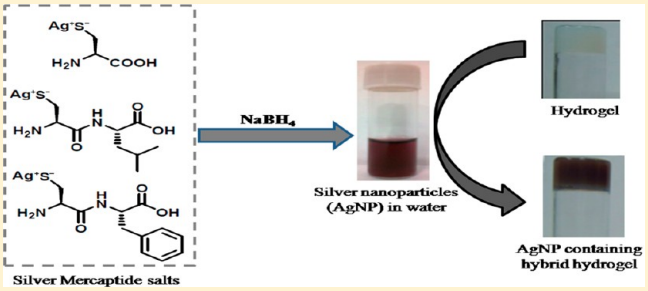

INTRODUCTION

Formation of supramolecular gels[1−18] from small organic molecules has attracted significant research interest over the past several years. Low molecular weight gelators are self-assembled using different kinds of noncovalent interactions including $\pi-\pi$ stacking, hydrogen bonding, hydrophobic, ionic, van der Waals, and others to form gels.[1−18] Hydrogel formation has often been triggered by different kinds of external stimuli, such as enzymes,[19,20] pH,[21,22] solvents,[23−25] metal ions,[26,27] salt concentrations,[28,29] and others. Adams and co-workers have recently developed a new technique to trigger the hydrogelation of several short peptides utilizing the hydrolysis of glucono-δ-lactone by controlling the pH of the medium.[30,31]Hydrogel materials have been extensively studied owing to their potent applications in vast areas, including sustained release of drugs and bioactive molecules,[24,32−34] scaffolds for tissue growth,[35,36] repair and wound healing,[37] catalysis of organic reactions,[38] pollutant removal from wastewater,[39−41] and others. Hamley[42−44]and co-workers have studied the self-assembly and hydrogelation of several model short peptide sequences of the amyloidal β-peptide.

Construction of a nanohybrid system using gel nanofibers and inorganic nanomaterials has become an active area of current research.[45−59] Our research group has been involved in the discovery and development of peptide-based supramolecular gels[11,24,39,40,47,48,59,63,64] and preparation of these gel-based different nanohybrid systems.[11,47,48] Incorporation of different nanomaterials into the supramolecular gel matrix can affect and modulate the properties of the native gel.[45−58] The hybrid gel can exhibit physicochemical properties that are interesting and different from that of the native gel. There are several reports on the modulation of the mechanical property of gel phase materials by incorporating different nanomaterials, including nanoparticles, carbon nanotubes, graphene, metal ions, and others.[11,26−29,50−58]

An increase in the inorganic salt concentration has also triggered the tuning of the mechanical strength of gel phase materials.[26−29] Inclusion of metal ions (coming from inorganic salts) generally screens the negative charge of carboxylate groups of the corresponding gelator in gelation, and this assists in the formation of a more rigid gel system.[27] Previously, Bhattacharya and co-workers examined the mechanical strength

Received: June 26, 2012
Revised: August 20, 2012

   dx.doi.org/10.1021/jp306262t | *J. Phys. Chem. B* XXXX, XXX, XXX−XXX

of hybrid gels by incorporating different ligand-capped gold nanoparticles into the native organogel matrix.[52,53] They reported that incorporation of gold nanoparticles into the gel matrix initially enhanced the rigidity of the hybrid gel. Then, rigidity of the hybrid gel was diminished with a further increase in the concentration of nanoparticles. According to them, the organization of the gel materials was perturbed in the accommodation of an increased number of nanoparticles, and as a consequence of that, gel rigidity was decreased.

Guerzo and co-workers[51] have also demonstrated that the stiffness of anthracene-based organogel has been gradually decreased upon the incorporation of long-chain thiol-capped gold nanoparticles. Han and co-workers showed that the incorporation of a graphene sheet into the copolymer-based hydrogel remarkably diminished the elastic modulus (G'); viscous modulus (G''); and finally, the strength of the gel.[57]

In the course of our investigation on self-assembly and gelation of peptide based molecules,[11,24,39,40,47,48,59,63] an N-terminally protected tripeptide (Boc-Phe-Phe-Ala−OH) has been discovered to form a translucent, self-supporting gel in a basic aqueous medium. Moreover, silver nanoparticles containing hybrid hydrogels have been prepared by incorporating different cysteine-based-ligand-capped AgNPs into the native hydrogel. Although the gel strength can be easily tunable by varying the gelator concentration,[63] in this study, we are curious to investigate an alternative way to modulate the gel strength without changing the concentration of the gelator. In this regard, AgNP-containing hybrid gels have been prepared to address the point, whether gel strength can be modulated by the incorporation of AgNPs into the hybrid gel, and if yes, to find out the factors that are responsible for governing the modulation of the gel strength using rheological experiments. Rheological investigations reveal that the mechanical strength of the hybrid hydrogel depends on the nature of the capping ligands of the silver nanoparticles, the size of the nanoparticles, and the amount of nanoparticles added into the native gel.

EXPERIMENTAL METHODS

Materials. L-Phenylalanine, L-alanine, L-cysteine, L-leucine, formic acid (HCOOH), Boc anhydride, *N*,*N*′-dicyclohexylcarbodiimide (DCC), 1-hydroxybenzotriazole (HOBt), sodium borohydride ($NaBH_4$), silver nitrate ($AgNO_3$), and triphenyl methanol were purchased from Sigma Chemicals. All other common solvents were purchased from SRL, India.

Synthesis of Gelator Peptide. Tripeptide was synthesized by the conventional solution phase method using the racemization-free fragment condensation strategy. The Boc group was used for the N-terminal protection, and the C-terminus was protected as a methyl ester. Coupling reactions were mediated by DCC/HOBt. The C-terminal methyl group was removed using aqueous sodium hydroxide. All intermediate compounds and final compounds were purified and characterized well by mass and NMR spectroscopy.

Boc-Phe-Phe-Ala−OMe. Our group reported the synthesis of Boc-Phe-Phe-Ala−OMe in a recent report.[11]

Gelator Peptide (Boc-Phe-Phe-Ala−OH). Boc-Phe-Phe-Ala−OMe (6.39 g, 15.0 mmol) was dissolved in 20 mL of MeOH, and then 10 mL of 1 M NaOH was added. The reaction mixture was then stirred, and the progress of saponification was monitored by thin layer chromatography. After 10 h, the methanol was removed under vacuum, the residue was placed in 50 mL of water and washed with diethyl ether (2 × 50 mL). After that, the pH of the aqueous layer was adjusted to pH 2 using 1 M HCl, and it was extracted with ethyl acetate (3 × 50 mL). The ethyl acetate extract was pooled, dried over anhydrous sodium sulfate, and evaporated in vacuum to yield a white solid sample. Yield: 5.34 g (12.9 mmol, 86.0%). ^{1}H NMR (300 MHz, DMSO-d_6, 25 °C, δ): 12.38 (1H, br.), 8.19 (1H, d, J = 7.5), 7.82 (1H, d, J = 7.9), 7.17−6.98 (10H, m), 6.77 (1H, d, J = 8.3), 4.49−4.47 (1H, m), 4.14−4.10 (1H, m), 4.02−3.99 (1H, m), 2.96−2.93 (1H, m), 2.74−2.51 (2H, m), 2.47−2.31 (1H, m), 1.16 (9H, s), 1.06−1.00 (3H, m). ^{13}C NMR (75 MHz, DMSO-d_6, 25 °C, δ): 174.5, 172.0, 171.9, 171.5, 171.3, 155.8, 155.6, 138.6, 138.4, 138.1, 130.0, 129.7, 128.5, 128.4, 126.8, 126.7, 78.7, 78.5, 53.8, 48.0, 38.3, 38.1, 37.9, 28.6, 17.7. Anal. calcd. for $C_{26}H_{33}N_3O_6$ (483.2369): C, 64.58; H, 6.88; N, 8.69. Found C, 64.55; H, 6.89; N, 8.67. HRMS (m/z): 506.3529 $[M + Na]^+$, 507.3451 $[M + Na + H]^+$.

Synthesis of Amino Acid/Dipeptide-Based Silver Mercaptides. Dipeptides were synthesized by conventional solution phase methodology by using the racemization-free fragment condensation strategy (Scheme S1, Supporting Information). The N-terminus was protected by the Boc group, the C-terminus was protected as a methyl ester, and the thiol (−SH) group was protected by the trityl group. Couplings were mediated by DCC/HOBt. Deprotection of the methyl ester was performed using the saponification method, deprotection of the Boc was performed by HCOOH, and deprotection of the trityl group was performed by treatment with $AgNO_3$ in the presence of pyridine. All compounds were characterized by mass spectrometry (HRMS) and ^{1}H NMR spectroscopy (300 MHz).

Hydrogel Preparation. A requisite amount of gelator peptide was taken in a screw-capped glass vial. Aqueous NaOH solution was then added into that glass vial. This resultant mixture was heated until the gelator molecules were dissolved completely, and this upon cooling at room temperature for 2 min gave a self-supported translucent hydrogel. This hydrogel is stable over 15 days at room temperature without any visual change.

INSTRUMENTATIONS

Field Emission Scanning Electron Microscopy (FE-SEM). FE-SEM experiments were performed by placing a small portion of gel samples on a microscope cover glass. These samples were then dried first in air and then in vacuum and coated with platinum for 90 s at 10 kV voltages and 10 μA current. The thickness of the coating layer of platinum was 3−4 nm. After that, micrographs were taken by using a SEM apparatus, Jeol scanning microscope JSM-6700F.

Transmission Electron Microscopy (TEM). Morphologies of native and hybrid hydrogels were studied using TEM experiments. A drop of dilute solution of the gel-phase material of the corresponding gel was placed on carbon coated copper grids (300 mesh) and dried by slow evaporation. Each grid was then allowed to dry in a vacuum at 30 °C for two days. Images were taken with an FEI (Tecnai Spirit) instrument.

Congo Red Binding Study. A 2.0% (w/v) hydrogel was prepared, and Congo red solution (1 mmol) was added into the gel vial. Congo red-stained hydrogel was then prepared by a heating−cooling cycle. This hydrogel was allowed to age for 1 day, and a small piece of the gel was taken out in a spatula, and this gel was placed on a glass side upon shearing. Excess dye was removed by washing using distilled water, then the sample was dried in vacuum at room temperature for 24 h. The dried

dx.doi.org/10.1021/jp306262t | J. Phys. Chem. B XXXX, XXX, XXX−XXX

gel sample was observed under a cross polarizing optical microscope (at 100× magnification).

X-ray Diffraction Study. Hydrogel was prepared at a concentration of 3.0% (w/v), and it was then subjected to lyophilization to obtain the xerogel sample. X-ray diffraction study of this xerogel was carried out by placing the sample on a glass plate. The experiment was carried out by using an X-ray diffractometer (Bruker AXS, model no. D8 Advance). The instrument was operated at a 40 kV voltage and 40 mA current using Ni-filtered Cu Kα radiation, and the instrument was calibrated with a standard Al_2O_3 (corundum) sample before use. For 5−30° scans, the LynxEye super speed detector was used with scan speed 0.3 s and step size 0.02°.

Differential Scanning Calorimetry (DSC). Thermal behavior of the gel was studied using a Perkin-Elmer differential scanning calorimeter (Diamond DSC-7) working under N_2 atmosphere. The gel sample was taken in a large volume capsule (LVC) tightly sealed with an O-ring. It was then heated from 20 to 90 °C at a heating rate of 5 °C/min. A cooling run was also taken after waiting 10 min at 90 °C, and then the sample was cooled to 20 °C at a rate of 2 °C/min. The instrument was calibrated with indium and cyclohexane.

FT-IR Study. FT-IR spectra were recorded using a Nicolate 380 FT-IR spectrophotometer (Thermo Scientific). The FT-IR spectrum of the gelator in solid and xerogel state (obtained from 3.0% (w/v) hydrogel) were recorded using the KBr disk technique. Xerogel was dissolved in D_2O to get the hydrogel (3.0%, w/v), and this wet gel was used for the FT-IR study using a CaF_2 cell.

Rheology. Rheological experiments were performed with an AR 2000 advanced rheometer (TA Instruments) using cone plate geometry in a Peltier plate. The cone diameter was 40 mm, the cone angle was 1° 59′ 50″, and truncation was 56 μm.

NMR Experiment. All NMR studies were carried out on a Brüker DPX 300 MHz spectrometer at 300 K using a cryo probe in $CDCl_3$ and DMSO-d_6 maintaining a concentration of 4−10 mM.

Mass Spectrometry. Mass spectra were recorded on a QTOF Micro YA263 high-resolution mass spectrometer.

RESULTS AND DISCUSSION

Gelation and Thermal Study. Hydrogenation depends upon the fine balance between hydrophobicity and hydrophilicity of the gelator molecule. This gelator molecule (Figure 1) contains two hydrophobic, aromatic phenylalanine (Phe) residues and one alanine residue, and its N-terminus is protected with a hydrophobic Boc group. However, this gelator molecule contains one hydrophilic −COOH group, and its protonation and deprotonation can be tuned by changing the pH of solution. Hydrogelation was achieved by dissolving the gelator peptide completely in a basic aqueous solution of sodium hydroxide upon heating. This resulting clear solution formed a stable opaque hydrogel upon cooling at room temperature for 2 min. Gel formation was checked by the test tube inversion method. This opaque hydrogel became translucent at lower concentration (Figure 2). The minimum gelation concentration (MGC) was 1.3% (w/v). Hydrogel is found to be thermoreversible in nature. Upon slow heating, the hydrogel became a sol (solution), whereas on cooling, the gelation property was regained. The gel melting temperature was measured by heating the hydrogel in a thermostat-controlled water bath until it had flown. The gel-to-sol transition temperature (T_{gel}) was plotted against the concentrations of the gelator peptide in Figure 3a. It was observed that initially, the T_{gel} value increased sharply and then, it increased slowly with the increasing concentration of the gelator peptide until a typical concentration regime was reached.[48] Further addition of gelator molecules failed to increase the T_{gel} significantly. This indicates that a "plateau region" was attained.[48] At minimum gelator concentration (MGC) 1.3% (w/v), the gel to sol transition took place at 48 °C.

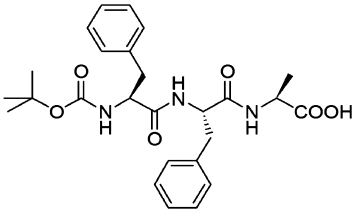

Figure 1. Chemical structure of N-terminally Boc-protected tripeptide-based hydrogelator.

Figure 2. Glass vial containing translucent hydrogel obtained from tripeptide.

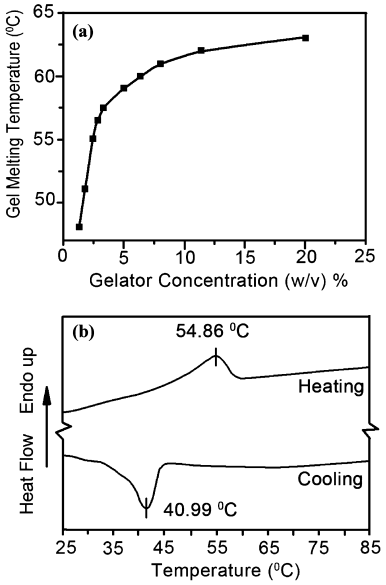

Figure 3. (a) Concentration−gel melting temperature phase diagram of hydrogel. (b) DSC thermogram of the hydrogelator at 2.5% (w/v).

A DSC experiment was performed to examine the thermoreversibility of the hydrogel materials (Figure 3b). The hydrogel has shown an endotherm on heating and an exotherm upon cooling. It has been observed that the gel-melting

dx.doi.org/10.1021/jp306262t | J. Phys. Chem. B XXXX, XXX, XXX−XXX

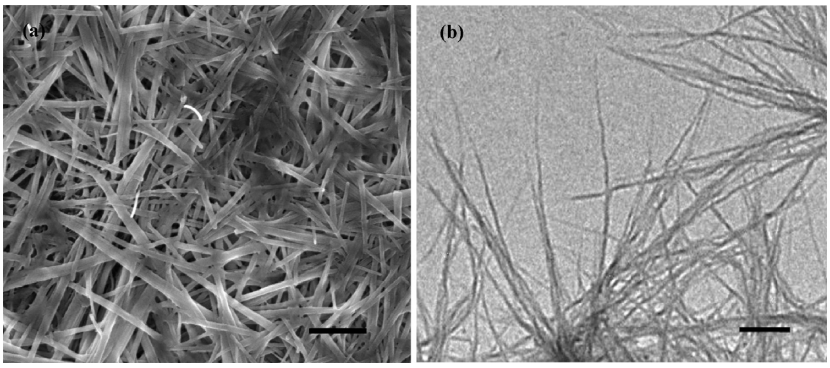

Figure 4. (a) FE-SEM image of xerogel obtained from the peptide based hydrogel showing nanofibrillar assemblies (scale bar = 1 μm) and (b) TEM image of this xerogel obtained hydrogel, also showing nanofibrillar assemblies, in an enlarged view (scale bar = 500 nm).

temperature (54.86 °C for 2.5% w/v gel) from the DSC thermogram in Figure 3b is comparable with the concentration−temperature phase diagram in Figure 3a. The temperature difference between the endotherm and exotherm is ∼15 °C, and this indicates hysterisis. This is a characteristic of a first-order phase transition.[59,60]

Morphological Study. Morphological study of the hydrogel was carried out using various electron microscopic experiments, including FE-SEM and TEM. The FE-SEM image (Figure 4a) of the xerogel obtained from the hydrogelator showed a nanofibrillar morphology with a high aspect ratio. Widths of the gel nanofibers range from 80 to 150 nm, and these nanofibers are several micrometers in length. The high aspect ratios of the gel nanofibers clearly indicate that the intermolecular interactions between the gelator molecules are highly anisotropic. Similarly, fibrillar nanostructures have also been observed from the TEM study (Figure 4b). Widths of these nanofibers are in the range of 30−60 nm, and these fibers are several micrometers in length.

Congo Red Binding Study. Our reported tripeptide is a part of the amyloid peptide sequence (Aβ,[19−21] Phe-Phe-Ala), so some properties of this amyloid peptide fragment can be similar to the native one.[61,62] Hydrogel containing this fragment was examined by staining with a physiological dye, Congo red. The dried gel material was viewed under a polarized microscope. The Congo red staining experiment showed a typical green-gold birefringence, indicating the characteristic feature of a native amyloid (Figure 5).[61,62] Congo red binding has usually been taken as a consideration for the amyloidogenic property. Moreover, it has been used sometimes as a probe for the formation of a β-sheet structure.[62]

FT-IR Study. Fourier transformed infrared (FT-IR) spectroscopy is a powerful tool for studying the structural aspects of the gelator peptide in the assembled gel state. FT-IR spectra of the gelator were taken in three different states: solid, wet gel, and xerogel states. In the solid state, a sharp peak at 1649 cm^{-1} is corresponding to the amide carbonyl (>C═O) stretching frequency. Peaks at 1548 and at 3299 cm^{-1} correspond to the N−H bending and N−H stretching frequencies of the gelator, respectively, in the solid state. Interestingly, the peak corresponding to the amide carbonyl (>C═O) stretching frequency of the gelator molecule in the xerogel state and also in the wet gel state appeared at 1635 cm^{-1}. The N−H bending frequency was shifted to 1529 and 1537 cm^{-1} for the xerogel and the wet gel states, respectively. This observation indicates that all N−H and >C═O are hydrogen bonded in the assembled gel state (in both xerogel and wet gel) and suggests

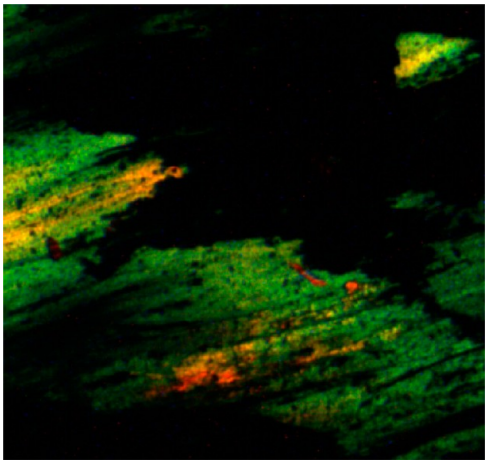

Figure 5. Polarizing optical microscopic image of dried hydrogel staining with a physiological dye Congo red showing an apple green birefringence.

that a β-sheet conformation is present in the assembled gel state.[40,48]

Moreover, weak bands at 1689 and at 1688 cm^{-1} were observed in the xerogel and wet gel states, respectively. This suggests the presence of an antiparallel β-sheet arrangement in the gel state.[40,48] In this system, hydrogelation has taken place in the carboxylate ($-COO^-$) form of the gelator molecule, and this has been supported by the change of the 1718 cm^{-1} peak (for carboxylic group) in the solid state to 1585 cm^{-1} and 1409 cm^{-1} for antisymmetric and symmetric stretching band, respectively, of the carboxylate group in the wet gel state (Figure 6b).[40] A similar observation was noticed in the xerogel state, suggesting the formation of a carboxylate ion in the gel state (Figure 6a).

XRD Study. X-ray diffraction (XRD) study of the xerogel was carried out to obtain information about the molecular packing of self-assembled peptides in the gel state (Figure S1, Supporting Information). The presence of a sharp peak at 2θ = 8.4° with a d spacing of 10.53 Å has been accompanied by another peak at 2θ = 18.15° with a d spacing value of 4.88 Å (Figure S1, Supporting Information). This indicates the presence of an antiparallel β-sheet structure in the xerogel state of the gelator.[48] A characteristic peak at 2θ = 23.4° with a d value of 3.7 Å is indicative of the $\pi-\pi$ stacking distance. This also suggests the presence of aromatic−aromatic interactions in the assembled gel state.[48]

dx.doi.org/10.1021/jp306262t | J. Phys. Chem. B XXXX, XXX, XXX−XXX

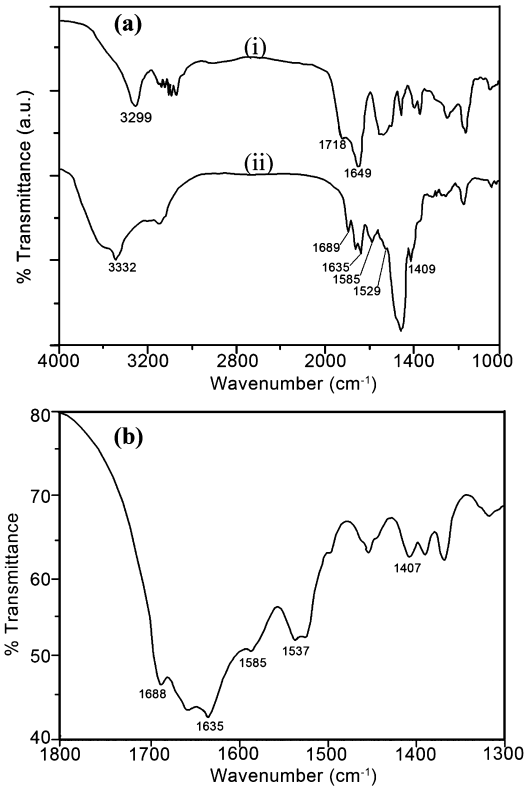

Figure 6. (a) FT-IR spectra of the gelator peptide (i) in the solid state and (ii) in the xerogel state and (b) FT-IR spectrum of the native wet gel state.

Rheological Study. Mechanical property of the hydrogel is important for determining its suitability in various applications. An oscillatory shear rheometer was used to probe the dynamic mechanical properties of gels. The storage modulus (measurement of elastic property) and loss modulus (measurement of fluidity of gel) are expressed as G' and G'', respectively. Theoretically, if $G'(\omega)$ is proportional to ω_0, $G''(\omega)$ is proportional to ω_0, and $G'(\omega) > G''(\omega)$ (at low frequency region), the system is considered to behave as a gel; where ω is the angular frequency.[59] In the sol state, loss modulus (G'') will be greater than storage modulus (G'). Rheometric parameters, storage modulus (G') and loss modulus (G'') are dependent on the concentration of the gelator, so the concentrations of all hydrogels were maintained at 3.0% (w/v). The storage and loss moduli of the hydrogel were measured at 27 °C after 20 min of the gel formation.

In a typical frequency sweep experiment, variations of storage modulus (G') and loss modulus (G'') were monitored as a function of the applied angular frequency under a fixed stress of 0.589. From Figure 7a, it has been noticed that the storage modulus has not crossed the loss modulus in the experimental regions, indicating the typical behavior of a gel phase material.[59,63,64,66−68] This gelator tripeptide forms a moderately rigid hydrogel with G' on the order of 10^4 Pa at the tested experimental frequency region. G' and G'' are also independent of frequency within the experimental limit (Figure 7a).

In another typical experiment, storage and loss moduli were measured with respect to the applied stress at a fixed strain 0.1% (Figure 7b).[69−72] It is evident from the Figure 7b that the storage modulus is higher than the loss modulus initially, and after a certain stress value, the storage modulus and loss modulus cross each other. This is called the yield stress (σ_y). In

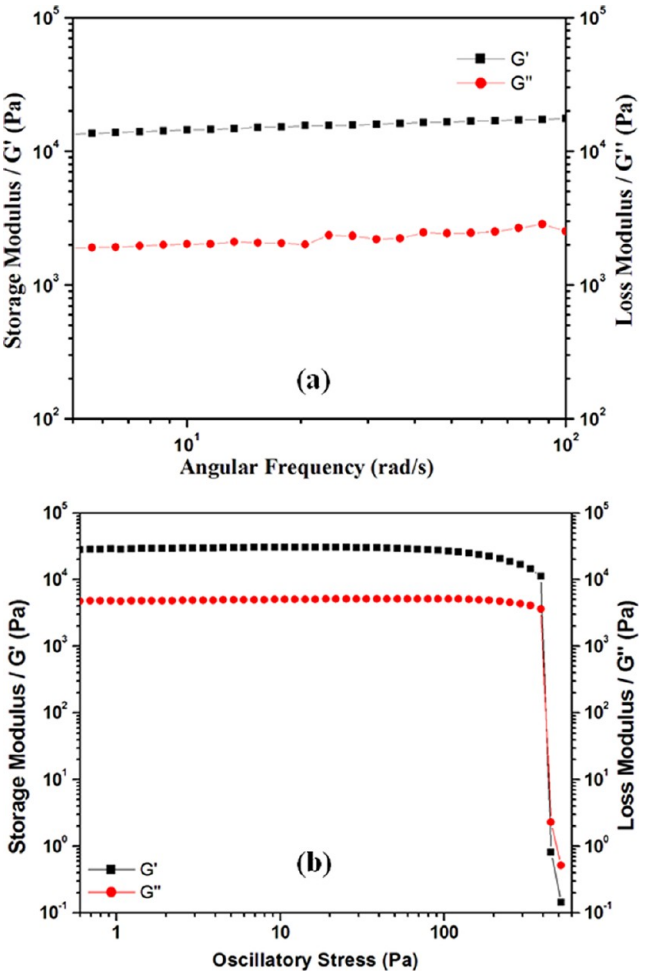

Figure 7. (a) Log−log plots of storage modulus and loss modulus versus the angular frequency of hydrogel (3.0% w/v) and (b) log−log plots of storage and loss modulus versus the applied stress of hydrogel (3.0% w/v).

this study, the calculated yield stress value was found to be 394.3 Pa. It implies the excellent rheological properties of this tripeptide-based hydrogel. Generally, the yield stress values of supramolecular hydrogel are less;[69−72] however, the yield stress value obtained from our tripeptide-based hydrogel is comparable to other supramolecular gels.[72] A high storage modulus (G') and high yield stress (σ_y) values indicate the formation of a significantly rigid gel material.

PREPARATION OF HYBRID HYDROGEL

Synthesis of Silver Nanoparticles (AgNPs). It is well-known that thiol (−SH) can stabilize silver nanoparticles very strongly.[73] In this study, the design of the capping ligands has been done in such a way that one part of the ligand (cysteine) can stabilize AgNPs and the other part can interact with the gelator peptide simultaneously. For this purpose, three different silver mercaptides of cysteine (1), cysteinyl leucine (2), and cysteinyl phenylalanine (3) were synthesized to prepare small silver nanoparticles (Scheme 1). Modification of capping ligands from the cysteine-to-cysteine-based dipeptides have been done keeping in mind that the presence of other amino acid residues (e.g., leucine) in Cys-Leu and phenylalanine in Cys-Phe residues can interact with the gelator peptide using hydrophobic/aromatic interactions.

dx.doi.org/10.1021/jp306262t | J. Phys. Chem. B XXXX, XXX, XXX−XXX

Scheme 1. Schematic Presentation for the One-Step Pot Synthesis of Silver Nanoparticles Using the Simple Reduction of Silver Mercaptides and Subsequent Incorporation of As-Prepared Silver Nanoparticles into the Hydrogel to Prepare Silver Nanoparticles Containing the Hybrid Hydrogel

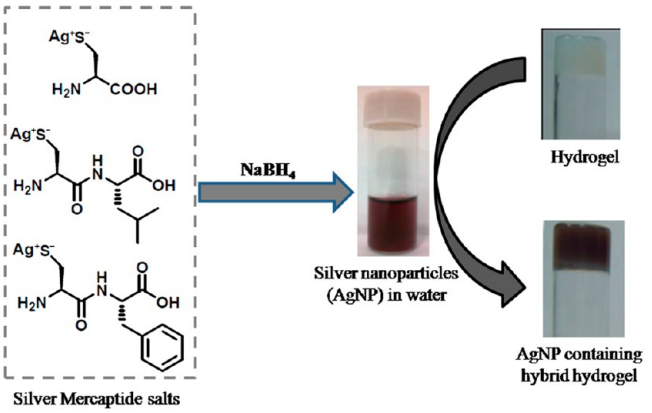

To prepare silver nanoparticles, as-prepared cysteine-based silver mercaptide were taken in glass vials and dispersed in water by sonication. Then an aqueous solution of $NaBH_4$ was added dropwise into this yellowish aqueous dispersion. Instantly, the color of the mixture changed to dark brown (Scheme 1). This is due to the formation of silver nanoparticles (AgNPs). The strong reducing agent sodium borohydride reduces Ag^+ to Ag^0. These silver mercaptide salts can serve as a good precursor for the preparation of small, homogeneous silver nanoparticles. The presence of an internal sulfur atom in these silver salts can stabilize the silver nanoparticles very well, and the presence of hydrophilic amino ($-NH_2$) and carboxylate ($-COO^-$) groups in the capping ligands helps to solubilize the silver nanoparticles in water.

These as-synthesized AgNPs from different mercaptide salts have been characterized by TEM studies (Figure 8) and energy dispersive X-ray (EDX) analysis (Figure S2, Supporting Information). Sizes of these as-prepared silver nanoparticles are small, and size distribution is almost homogeneous (Figure 8). The size of the as-synthesized silver nanoparticles gradually decreases with the capping ligand 1 to 2 to 3. The AgNPs obtained from the Cys (ligand 1)-capped mercaptide salts are relatively larger in size and less homogeneous in size distribution than those of AgNPs stabilized by the ligand 2 or 3. The average diameter of Cys (ligand 1)-capped nanoparticles is 4.5 nm; however, the average diameters of ligand 2 (Cys-Leu)- and ligand 3 (Cys-Phe)-capped AgNPs are 3.2 and 2.4 nm, respectively. So, different capping ligands can influence the size of AgNPs, and the size of Ag nanoparticles with different capping ligands follows the following order Cys-Phe < Cys-Leu < Cys.

Hybrid Hydrogels. Gel materials were heated to melt into the sol (solution) phase, and then the requisite amount of AgNPs [capped with three different ligands: Cys (1), Cys-Leu (2), Cys-Phe (3)] were added separately to the sol. In each case, the gelator concentration was kept fixed at 3.0% (w/v). Finally, these mixtures were heated and shaken well to produce

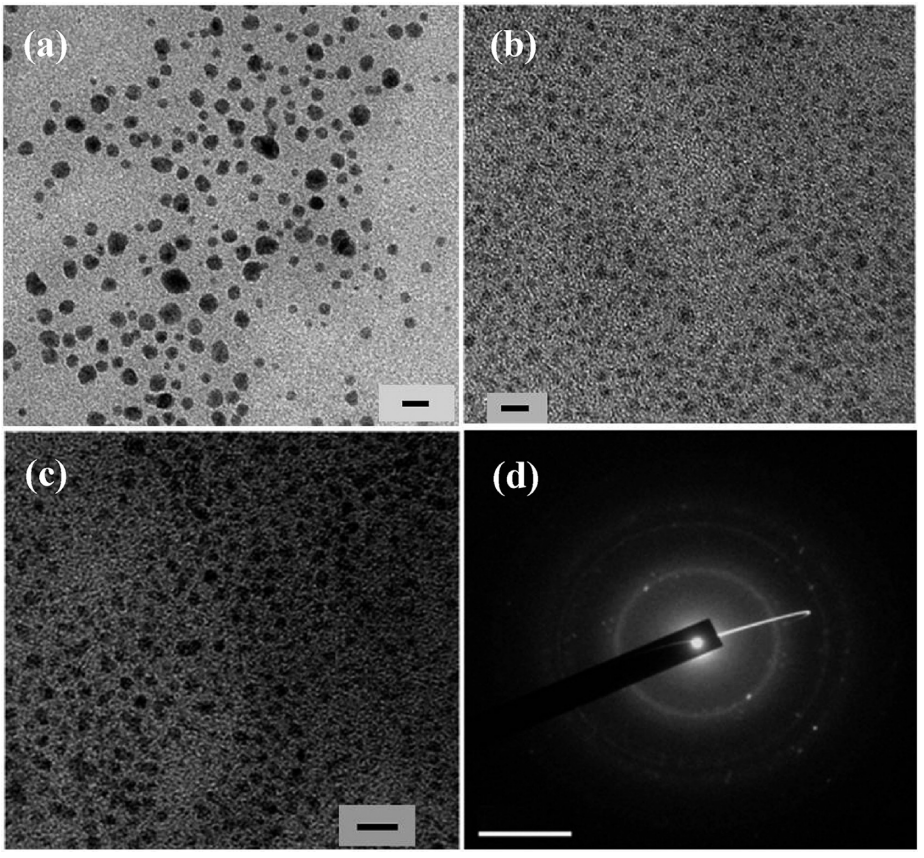

Figure 8. TEM images of different AgNPs capped with (a) Cys (1), (b) Cys-Leu (2) and (c) Cys-Phe (3) ligands, respectively (scale bar = 10 nm) and (d) selected area diffraction pattern of Cys (ligand 1)-capped silver nanoparticles (scale bar = 5 nm^{-1}).

dx.doi.org/10.1021/jp306262t | J. Phys. Chem. B XXXX, XXX, XXX–XXX

homogeneous sols. These silver nanoparticles containing homogeneous colloidal dispersions upon cooling at room temperature give a self-supported hybrid hydrogel. Figure 9 shows photographs of these hybrid hydrogels containing silver nanoparticles in various molar ratios with respect to the peptide gelator.

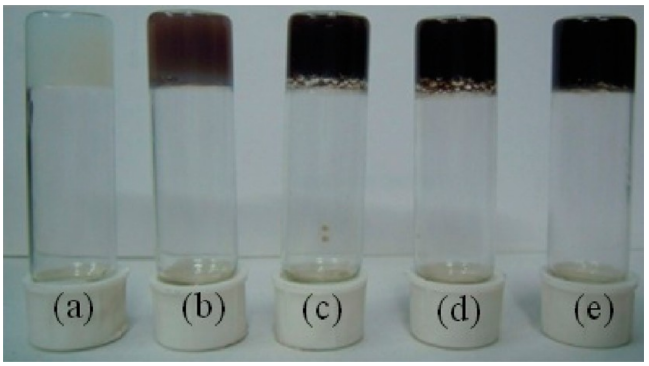

Figure 9. Photographs of silver nanoparticles containing hybrid hydrogel at different molar ratios with respect to the gelator (a) without silver nanoparticles, (b) 100:1, (c) 100:3, (d) 100:5, and (e) 100:15.

The morphology of the hybrid gel (having Cys-Phe-capped Ag NPs) has been studied using TEM experiments (Figure 10).

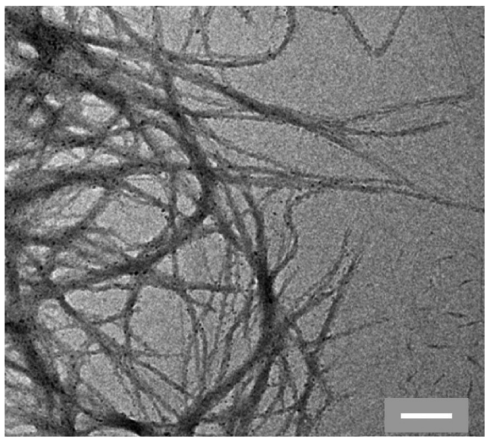

Figure 10. TEM images of Cys-Phe (3)-capped AgNPs doped composite hydrogel (nanoparticles to hydrogelator molar ratio 5:100). The black dots indicate silver nanoparticles and these nanoparticles are mainly deposited on the gel nanofibers. The scale bar is 250 nm.

The TEM image (Figure 10) exhibits that the fabrication of silver nanoparticles is mainly along the gel nanofibers and they are rarely present outside these gel nanofibers. Fabrication of these AgNPs is due to noncovalent (hydrogen bonding, van der Waal, and $\pi-\pi$ interactions) interactions between the ligand (Cys/Cys-Leu/Cys-Phe)-capped silver nanoparticles and tripeptide-based hydrogel nanofibers. EDX analysis (Figure S3, Supporting Information) shows that these black dots are due to the presence of AgNPs within the hybrid hydrogel.

Rheological Study of Hybrid Hydrogels. Silver nanoparticles (AgNPs) are fabricated along the gel nanofibers (Figure 10). This result indicates that nanoparticles interact with the gelator network, and these interactions of nanoparticles with different capping ligands can also influence the gelator's self-assembly. Rheological studies of these hybrid hydrogels can shed light on the interaction between the nanoparticle and the gel nanofiber.[51−53] These observations motivated us to perform rheological studies of hybrid hydrogels for examining the influence of the hybrid gel strength on the incorporation of AgNPs within the hydrogel matrix. To study the role of the concentration of the nanoparticles in the mechanical strengths of the hybrid hydrogels, four different sets of hybrid hydrogels were prepared by varying the concentration of the nanoparticles. These nanoparticles were synthesized from a particular mercaptide salt (Cys-Phe) with the following nanoparticle-to-hydrogelator molar ratios: 1:100, 3:100, 5:100, and 15:100.

Oscillatory stress sweep experiments (Figure 11) were performed on hybrid hydrogels with different amounts of

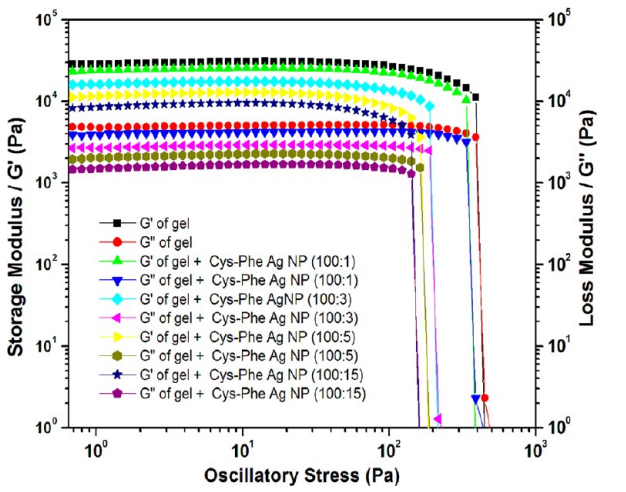

Figure 11. Comparative oscillatory stress sweep experiments of the tripeptide-based native hydrogel (3% w/v) and silver nanoparticles containing hybrid hydrogels (doped with Cys-Phe-capped AgNPs) having gelator to AgNPs molar ratios of 100:1, 100:3, 100:5, and 100:15, respectively.

AgNPs at 27 °C at a constant strain of 0.1%. The yield stress values (σ_y) and the storage modulus values at oscillatory stress 1.06 Pa of native and hybrid hydrogels are summarized in Table 1. From this table, it is clear that the storage modulus and the

Table 1. Storage Modulus (at oscillatory stress 1.06 Pa) and Yield Stress Values of the Native Hydrogel and Hybrid Hydrogels after Doping by the Cys-Phe (ligand 3)-Capped Silver Nanoparticles at Different Molar Ratios

gels	G' (Pa)	yield stress (σ_y) (Pa)
native gel	28 098	390.7
gel/AgNP (100:1)	24 165	334
gel/AgNP (100:3)	15 960	190.6
gel/AgNP (100:5)	11 367	162
gel/AgNP (100:15)	8 407	140

yield stress values for these hybrid hydrogels are less than that of the native hydrogel. For four different sets of hybrid hydrogels, storage moduli and the yield stress values gradually decreased with an increase in the concentration of silver nanoparticles (Figure 11).

Another set of rheological experiments was performed on three different hybrid hydrogels that were prepared by doping three different ligand [Cys (1), Cys-Leu (2), and Cys-Phe (3)]-

dx.doi.org/10.1021/jp306262t | J. Phys. Chem. B XXXX, XXX, XXX−XXX

stabilized AgNPs (Figure 12). These studies were performed to investigate the role of different capping ligands in the hybrid

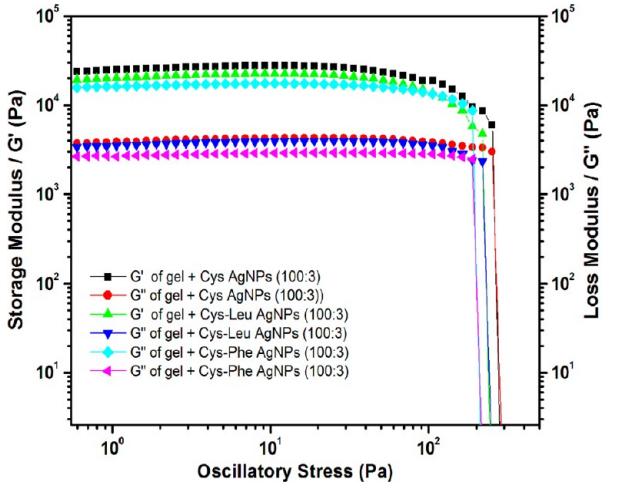

Figure 12. Comparative oscillatory stress sweep experiments of the tripeptide-based hydrogels (3.0% w/v) containing silver nanoparticles with different capping ligands (Cys, Cys-Leu, and Cys-Phe). In all these hybrid hydrogels, the molar ratio of the gelator to silver nanoparticles was maintained at 100:3.

hydrogel. These hybrid hydrogels were prepared by fixing the molar ratio of the gelator to the AgNPs at 100:3. Figure 12 shows that the storage modulus and also the yield stress values of three hybrid hydrogels are less than that of the native gel (Table 2). The storage modulus and yield stress values of

Table 2. Storage Modulus (at oscillatory stress 1.06 pa) and Yield Stress Values of Different Ligand Capped Silver Nanoparticles at 100:3 Molar Ratio

gels	G' (Pa)	yield stress (σ_y) (Pa)
Cys AgNP	25 083	253
Cys-Leu AgNP	20 181	218
Cys-Phe AgNP	15 960	190.6

hybrid hydrogels for the three different capping ligands follow the following order Cys (1) > Cys-Leu (2) > Cys-Phe (3). It can be stated that the incorporation of amino acid/peptide-capped AgNPs into the hydrogel lowers the mechanical strength of the gel matrix. The destabilizing effect of the Cys-Phe (3)-capped AgNPs in the hydrogel matrix is the maximum, whereas the destabilizing effect of Cys-Leu (2) ligand is medium, and the destabilizing effect of the Cys (1) ligand is the least.

In our study, the overall morphology of the gel nanofibers has not been altered after incorporation of the silver nanoparticles within the hydrogel matrix. From the TEM image, it is evident that cysteine-based ligand-capped silver nanoparticles are fabricated along the gel nanofibers. The presence of an amino acid/dipeptide functionality in a nanoparticle can interact with the peptide-based hydrogel nanofibers. These interactions present between the gel nanofibers and ligand-capped nanoparticles are noncovalent.[48] Incorporation of metal nanoparticles can either increase or decrease the stiffness of the resulting hybrid gel. There are two possibilities: (a) the noncovalent interactions between nanoparticles and gelators can favor gelator−gelator interactions, and thereby, the mechanical strength of the hybrid hydrogel can be increased more than that of the native hydrogel; (b) the noncovalent interactions between nanoparticles and gelator molecules can disfavor the gelator−gelator interactions and, thereby, their assembly. Hence, the mechanical strength of the hybrid hydrogel may be diminished compared with that of the native gel.

Incorporation of AgNPs (capped with different ligands) within the hydrogel matrix causes the lowering of the mechanical strength of the hybrid gels than that of the native gel. We believe that noncovalent interactions (hydrogen bonding, van der Waals, and aromatic interactions) between the amino acid/peptide-capped silver nanoparticles and gelator can disfavor the self-assembly of gelator molecules to some extent within the hybrid hydrogel. This can cause the lowering of the mechanical strength of the hybrid hydrogel. It can be noted that a peptide-based gelator contains amide and hydrophobic/aromatic moieties (Figure 1). On the other hand, nanoparticle stabilizing/capping ligands (amino acid/peptide) also have hydrogen bonding or hydrophobic/aromatic functionalities (or both). Therefore, it is expected that nanoparticle stabilizing ligands can interact strongly with the peptidic gelator using various noncovalent interactions. Ligand 1 (Cys) has only two hydrogen bonding functionalities ($-NH_2$ and −COOH), whereas ligands 2 and 3 have a larger number of hydrogen bonding functionalities than ligand 1, because both have one extra amide group in their respective structures. Moreover, ligand 3 (Cys-Phe) has one aromatic moiety, which can participate in $\pi-\pi$ interactions with the gelator molecules, and ligand 2 (Cys-Leu) is devoid of any such type of aromatic moiety in its side chain. So, the increase in functionalities can help the interactions among the capping ligands of nanoparticles and gelator molecules, and this can weaken the assembly of gelator molecules by disfavoring the interactions among gelator molecules to some extent (Figure S4, Supporting Information). This can explain the observation that the storage modulus value and yield stress values of the Cys-Leu/Cys-Phe (ligands 2/3)-capped AgNP-doped hybrid hydrogel are less than that of the Cys (ligand 1)-capped silver nanoparticle-doped hybrid hydrogel (Table 2). Further replacement of amino acid residue Leu (in ligand 2) by the amino acid residue Phe (in ligand 3) introduces an aromatic functionality, and this functionality can interact with the gelator peptide (containing two Phe residues) using $\pi-\pi$ interactions. This results in more weakening of the gelator−gelator interactions for the ligand 3-capped AgNPs than that of the ligand 2 capped AgNPs (Figure S4, Supporting Information). As a consequence, the mechanical strength of the hybrid hydrogel containing ligand 3-stabilized AgNPs is less than that of the ligand 2-capped AgNPs.

Differences in sizes of AgNPs (capped with three different ligands) may be another reason for the variation of the mechanical strength of different AgNPs containing hybrid gels. It is evident from the TEM image (Figure 8) that the average size of AgNPs is gradually decreased with the capping ligands 1 to 2 to 3. It is expected that the surface area will be higher for smaller particles than that of the larger particles, so in this case, the interacting surface area between the different ligand-capped AgNPs and gel nanofibers follow the following order: Cys (1) < Cys-Leu (2) < Cys-Phe (3). Therefore, it can be stated that the more the interacting surface area of AgNPs, the more the unfavoring interactions among the gelator molecules. This causes an effect of the lowering of the gel strength in the

dx.doi.org/10.1021/jp306262t | J. Phys. Chem. B XXXX, XXX, XXX−XXX

following order: Cys (1) > Cys-Leu (2) > Cys-Phe. This is evident from the rheological study of hybrid hydrogels and the native gel.

CONCLUSION

A tripeptide-based, self-supporting, translucent hydrogel has been discovered. This gel phase material has been well characterized morphologically (FE-SEM and TEM), structurally (FT-IR, XRD, DSC), and rheologically. Cysteine and different synthetic dipeptides containing a cysteine residue have been used to make very small and almost homogeneous AgNPs, and these AgNPs have been incorporated into the native hydrogel matrix to prepare silver nanoparticle-containing hybrid hydrogel materials. Morphological study (using TEM) of the hybrid hydrogel has shown the fabrication of silver nanoparticles along the hydrogel nanofibers. Interestingly, the mechanical properties of the hybrid hydrogels have been successfully modulated by the inclusion of different ligand-capped silver nanoparticles. Different stabilizing ligands for the silver nanoparticles, size of the silver nanoparticles, and amount of the silver nanoparticles used in making the hybrid gels have definite roles in modulating the mechanical strength of these hybrid gels. Modulation of the gel strength by manipulating the noncovalent interactions in the supramolecular gel system has a significant implication in soft materials. Tuning of the strength of the hydrogel by altering the capping ligands for metal nanoparticles in a hybrid hydrogel system holds future promise to make new shear-responsive and smart biomaterials.

ASSOCIATED CONTENT

Supporting Information

Supporting Information contains XRD data of the xerogel, EDX analysis of the AgNPs and hybrid hydrogel, a tentative model indicating the mode of interactions of the gelator molecules and gelators and dipeptide-capped silver nanoparticles, characterization data of mercaptide salts, and spectra of gelator and mercaptide salts. This material is available free of charge via the Internet at http://pubs.acs.org.

AUTHOR INFORMATION

Corresponding Author

*Tel: +91-332473-4971. Fax: (+91) 332473-2805. E-mail: bcab@iacs.res.in, arindamkol1966@gmail.com.

Notes

The authors declare no competing financial interest.

ACKNOWLEDGMENTS

J.N., B.A., and S.B. acknowledge CSIR, New Delhi, India for their Senior Research Fellowship. We also acknowledge the support by the DST, India, Project No. SR/S1/OC-73/2009.

REFERENCES

(1) Terech, P.; Weiss, R. G. *Chem. Rev.* **1997**, *97*, 3133−3159.
(2) Sangeetha, N. M.; Maitra, U. *Chem. Soc. Rev.* **2005**, *34*, 821−836.
(3) Banerjee, S.; Das, R. K.; Maitra, U. *J. Mater. Chem.* **2009**, *19*, 6649−6687.
(4) Dawn, A.; Shiraki, T.; Haraguchi, S.; Tamaru, S.-i.; Shinkai, S. *Chem. Asian J.* **2011**, *6*, 266−282.
(5) Bhattacharya, S.; Samanta, S. K. *Langmuir* **2009**, *25*, 8378−8381.
(6) Jadhav, S. R.; Vemula, P. K.; Kumar, R.; Raghavan, S. R.; John, G. *Angew. Chem., Int. Ed.* **2010**, *49*, 7695−7698.
(7) Adams, D. J.; Topham, P. D. *Soft Matter* **2010**, *6*, 3707−3721.
(8) Ryan, D. M.; Nilsson, B. L. *Polym. Chem.* **2012**, *3*, 18−33.
(9) Adams, D. J. *Macromol. Biosci.* **2011**, *11*, 160−173.
(10) Gao, Y.; Zhao, F.; Wang, Q.; Zhang, Y.; Xu, B. *Chem. Soc. Rev.* **2010**, *39*, 3425−3433.
(11) Adhikari, B.; Nanda, J.; Banerjee, A. *Chem.—Eur. J.* **2011**, *17*, 11488−11496.
(12) Zhang, Y.; Kuang, Y.; Gao, Y.; Xu, B. *Langmuir* **2011**, *27*, 529−537.
(13) Mukhopadhyay, S.; Maitra, U.; Ira; Krishnamoorthy, G.; Schmidt, J.; Talmon, Y. *J. Am. Chem. Soc.* **2004**, *126*, 15905−15914.
(14) Hirst, A. R.; Escuder, B.; Miravet, J. F.; Smith, D. K. *Angew. Chem., Int. Ed.* **2008**, *47*, 8002−8018.
(15) Ajayaghosh, A.; Praveen, V. K.; Vijayakumar, C. *Chem. Soc. Rev.* **2008**, *37*, 109−122.
(16) Smith, D. K. *Chem. Soc. Rev.* **2009**, *38*, 684−694.
(17) Jayawarna, V.; Ali, M.; Jowitt, T. A.; Miller, A. F.; Saiani, A.; Gough, J. E.; Ulijn, R. V. *Adv. Mater.* **2006**, *18*, 611−614.
(18) Das, A. K.; Collins, R.; Ulijn, R. V. *Small* **2008**, *4*, 279−287.
(19) Gao, J.; Wang, H.; Wang, L.; Wang, J.; Kong, D.; Yang, Z. *J. Am. Chem. Soc.* **2009**, *131*, 11286−11287.
(20) Yang, Z.; Xu, B. *Adv. Mater.* **2006**, *18*, 3043−3046.
(21) Wang, T.; Jiang, J.; Liu, Y.; Li, Z.; Liu, M. *Langmuir* **2010**, *26*, 18694−18700.
(22) Zhao, Y.; Yokoi, H.; Tanaka, M.; Kinoshita, T.; Tan, T. *Biomacromolecules* **2008**, *9*, 1511−1518.
(23) Orbach, R.; Adler-Abramovich, L.; Zigerson, S.; Mironi-Harpaz, I.; Seliktar, D.; Gazit, E. *Biomacromolecules* **2009**, *10*, 2646−2651.
(24) Nanda, J.; Banerjee, A. *Soft Matter* **2012**, *8*, 3380−3386.
(25) Mahler, A.; Reches, M.; Rechter, M.; Cohen, S.; Gazit, E. *Adv. Mater.* **2006**, *18*, 1365−1370.
(26) Micklitsch, C. M.; Knerr, P. J.; Branco, M. C.; Nagarkar, R.; Pochan, D. J.; Schneider, J. P. *Angew. Chem., Int. Ed.* **2011**, *50*, 1577−1579.
(27) Chen, L.; Pont, G.; Morris, K.; Lotze, G.; Squires, A.; Serpell, L. C.; Adams, D. J. *Chem. Commun.* **2011**, *47*, 12071−12073.
(28) Shi, J.; Gao, Y.; Zhang, Y.; Pan, Y.; Xu, B. *Langmuir* **2011**, *27*, 14425−14431.
(29) Castelletto, V.; Hamley, I. W.; Cenker, C.; Olsson, U. *J. Phys. Chem. B* **2010**, *114*, 8002−8008.
(30) Sutton, S.; Campbell, N. L.; Cooper, A. I.; Kirkland, M.; Frith, W. J.; Adams, D. J. *Langmuir* **2009**, *25*, 10285−10291.
(31) Chen, L.; Morris, K.; Laybourn, A.; Elias, D.; Hicks, M. R.; Rodger, A.; Serpell, L.; Adams, D. J. *Langmuir* **2010**, *26*, 5232−5242.
(32) Wang, J.; Wang, Z.; Gao, J.; Wang, L.; Yang, Z.; Kong, D.; Yang, Z. *J. Mater. Chem.* **2009**, *19*, 7892−7896.
(33) Naskar, J.; Palui, G.; Banerjee, A. *J. Phys. Chem. B* **2009**, *113*, 11787−11792.
(34) Liang, G.; Yang, Z.; Zhang, R.; Li, L.; Fan, Y.; Kuang, Y.; Gao, Y.; Wang, T.; Lu, W. W.; Xu, B. *Langmuir* **2009**, *25*, 8419−8422.
(35) Zhou, M.; Smith, A. M.; Das, A. K.; Hodson, N. W.; Collins, R. F.; Ulijn, R. V.; Gough, J. E. *Biomaterials* **2009**, *30*, 2523−2530.
(36) Jayawarna, V.; Richardson, S. M.; Hirst, A. R.; Hodson, N. W.; Saiani, A.; Gough, J. E.; Ulijn, R. V. *Acta Biomater.* **2009**, *5*, 934−943.
(37) Yang, Z.; Liang, G.; Ma, M.; Abbah, A. S.; Lu, W. W.; Xu, B. *Chem. Commun.* **2007**, 843−845.
(38) Rodríguez-Llansola, F.; Miravet, J. F.; Escuder, B. *Chem. Commun.* **2009**, 7303−7305.
(39) Basak, S.; Nanda, J.; Banerjee, A. *J. Mater. Chem.* **2012**, *22*, 11658−11664.
(40) Adhikari, B.; Palui, G.; Banerjee, A. *Soft Matter* **2009**, *5*, 3452−3460.
(41) Rodríguez-Llansola, F.; Escuder, B.; Miravet, J. F.; Hermida-Merino, D.; Hamley, I. W.; Cardin, C. J.; Hayes, W. *Chem. Commun.* **2010**, *46*, 7960−7962.
(42) Castelletto, V.; Hamley, I. W.; Hule, R. A.; Pochan, D. J. *Angew. Chem., Int. Ed.* **2009**, *48*, 2317−2320.
(43) Hamley, I. W.; Brown, G. D.; Castelletto, V.; Cheng, G.; Venanzi, M.; Caruso, M.; Placidi, E.; Aleman, C.; Revilla-López, G.; Zanuy, D. *J. Phys. Chem. B* **2010**, *114*, 10674−10683.

(44) Cheng, G.; Castelletto, V.; Moulton, C. M.; Newby, G. E.; Hamley, I. W. *Langmuir* **2010**, *26*, 4990−4998.
(45) Coates, I. A.; Smith, D. K. *J. Mater. Chem.* **2010**, *20*, 6696−6702.
(46) Bhat, S.; Maitra, U. *Chem. Mater.* **2006**, *18*, 4224−4226.
(47) Ray, S.; Das, A. K.; Banerjee, A. *Chem. Commun.* **2006**, 2816−2818.
(48) Palui, G.; Nanda, J.; Ray, S.; Banerjee, A. *Chem.—Eur. J.* **2009**, *15*, 6902−6909.
(49) van Herrikhuyzen, J.; George, S. J.; Vos, M. R. J.; Sommerdijk, N. A. J. M.; Ajayaghosh, A.; Meskers, S. C. J.; Schenning, A. P. H. J. *Angew. Chem., Int. Ed.* **2007**, *46*, 1825−1828.
(50) Das, R. K.; Bhat, S.; Banerjee, S.; Aymonier, C.; Loppinet-Serani, A.; Terech, P.; Maitra, U.; Raffy, G.; Desvergne, J.-P.; Guerzo, A. D. *J. Mater. Chem.* **2011**, *21*, 2740−2750.
(51) Sangeetha, N. M.; Bhat, S.; Raffy, G.; Belin, C.; Loppinet-Serani, A.; Aymonier, C.; Terech, P.; Maitra, U.; Desvergne, J.-P.; Guerzo, A. D. *Chem. Mater.* **2009**, *21*, 3424−3432.
(52) Bhattacharya, S.; Srivastava, A.; Pal, A. *Angew. Chem., Int. Ed.* **2006**, *45*, 2934−2937.
(53) Pal, A.; Srivastava, A.; Bhattacharya, S. *Chem.—Eur. J.* **2009**, *15*, 9169−9182.
(54) Samanta, S. K.; Gomathi, A.; Bhattacharya, S.; Rao, C. N. R. *Langmuir* **2010**, *26*, 12230−12236.
(55) Samanta, S. K.; Pal, A.; Bhattacharya, S.; Rao, C. N. R. *J. Mater. Chem.* **2010**, *20*, 6881−6890.
(56) Moniruzzaman, M.; Sahin, A.; Winey, K. I. *Carbon* **2009**, *47*, 645−650.
(57) Zu, S.-Z.; Han, B.-H. *J. Phys. Chem. C* **2009**, *113*, 13651−13657.
(58) Srinivasan, S.; Babu, S. S.; Praveen, V. K.; Ajayaghosh, A. *Angew. Chem., Int. Ed.* **2008**, *47*, 5746−5749.
(59) Palui, G.; Garai, A.; Nanda, J.; Nandi, A. K.; Banerjee, A. *J. Phys. Chem. B* **2010**, *114*, 1249−1256.
(60) Raghavan, S. R.; Cipriano, B. H. Weiss, R. G.; Terech, P., Eds.; *Molecular Gels: Materials with Self-Assembled Fibrillar Networks*; Springer: Dordrecht, 2005, pp 233−244.
(61) Naskar, J.; Drew, M. G. B.; Deb, I.; Das, S.; Banerjee, A. *Org. Lett.* **2008**, *10*, 2625−2628.
(62) Ray, S.; Das, A. K.; Drew, M. G. B.; Banerjee, A. *Chem. Commun.* **2006**, 4230−4232.
(63) Adhikari, B.; Nanda, J.; Banerjee, A. *Soft Matter* **2011**, *7*, 8913−8922.
(64) Roy, S.; Banerjee, A. *Soft Matter* **2011**, *7*, 5300−5308.
(65) O'Leary, L. E. R.; Fallas, J. A.; Bakota, E. L.; Kang, M. K.; Hartgerink, J. D. *Nat. Chem.* **2011**, *3*, 821−828.
(66) Saha, A.; Roy, B.; Garai, A.; Nandi, A. K. *Langmuir* **2009**, *25*, 8457−8461.
(67) Bairi, P.; Roy, B.; Nandi, A. K. *J. Phys. Chem. B* **2010**, *114*, 11454−11461.
(68) Pal, A.; Dey, J. *Soft Matter* **2011**, *7*, 10369−10376.
(69) Patra, T.; Pal, A.; Dey, J. *Langmuir* **2010**, *26*, 7761−7767.
(70) Piepenbrock, M.-O. M.; Clarke, N.; Foster, J. A.; Steed, J. W. *Chem. Commun.* **2011**, *47*, 2095−2097.
(71) Bairi, P.; Roy, B.; Nandi, A. K. *RSC Advances* **2012**, *2*, 264−272.
(72) Molla, M. R.; Ghosh, S. *Chem. Mater.* **2011**, *23*, 95−105.
(73) Bhat, S.; Maitra, U. *J. Chem. Sci.* **2008**, *120*, 507−513.